

# Experimental Study On The Cold Flow Behaviour Of Azadirachta Indica (NEEM) Biodiesel Blended With Petroleum-based Fuels And Natural Organic Solvents

Mehmood Ali<sup>1\*</sup>, Amtul Qayoom<sup>2</sup>, Zehra Ghulam<sup>2</sup>, Shahab Imran<sup>3</sup>, MNAM Yusoff<sup>3</sup>, M.A. Kalam<sup>4</sup>, Omar Mahmoud<sup>5</sup>, and A.S. El-Shafay<sup>6</sup>

<sup>1</sup> Department of Environmental Engineering, NED University of Engineering and Technology, Karachi-75270, Pakistan

<sup>2</sup> Department of Chemistry, NED University of Engineering and Technology, Karachi-75270, Pakistan

<sup>3</sup> Centre of Energy Science, Department of Mechanical Engineering, University of Malaya, Kuala Lumpur 50603, Malaysia

<sup>4</sup> University of Technology Sydney, Australia

<sup>5</sup> Petroleum Engineering, Faculty of Engineering and Technology, Future University in Egypt, New Cairo 11845, Egypt

<sup>6</sup> Department of Mechanical Engineering, College of Engineering, Prince Sattam bin Abdulaziz University, Alkharj, 16273, Saudi Arabia

\* Corresponding author. E-mail: mehmood@neduet.edu.pk

Received: Apr. 08, 2022; Accepted: June 14, 2022

Due to the poor cold flow behaviour of biodiesel in winter, it tends to form solidifying gel in many cold regions across the world, making it challenging to use as an alternative fuel in diesel engines. This research investigation was conducted to investigate the comparative impact on cold flow parameters of biodiesel produced from Azadirachta indica (Neem oil) by blending with petroleum-based fuels and natural organic solvents. The B20 blends with kerosene showed significant improvement in CP, PP, and CFPP to -10 °C, -19 °C, and -20 °C, respectively. B20\* blend enhanced the CP, PP and CFPP to 8 °C, 2 °C, and 6 °C respectively, while mixed kerosene/ diesel B20\*\* blend improved CFPP, CP and PP by -4.5 °C, -7 °C and -8 °C respectively. Blend (B20T10) with natural turpentine oil improved CP, PP, and CFPP to 7 °C, 5 °C, and -2 °C, respectively. Diethyl ether and n-butanol did not show substantial improvement in biodiesel cold flow characteristics. The ester functional group in the biodiesel from ATR-FTIR spectral peaks was found at 1740.2 cm<sup>-1</sup> denotes C=O, i.e., carbonyl group confirmation in the presence of ester linkage. The cost analysis of B20y\*\* and B20T10 were found to be USD 0.747 and USD 0.782 per L, respectively in comparison to that of petroleum diesel, USD 0.770 per L. Neem biodiesel production showed a positive net energy balance of 14.28%. According to the current study, it is recommended to use blended mixed kerosene/diesel (B20\*\*) and biodiesel blend with turpentine oil (B20T10) in diesel engines with suitable physico-chemical and cold flow properties in compliance with ASTM D6571 standard.

**Keywords:** Biodiesel; Turpentine oil; Cold flow properties; Azadirachta indica; Kerosene; *n-butanol*

© The Author(s). This is an open access article distributed under the terms of the [Creative Commons Attribution License \(CC BY 4.0\)](https://creativecommons.org/licenses/by/4.0/), which permits unrestricted use, distribution, and reproduction in any medium, provided the original author and source are cited.

[http://dx.doi.org/10.6180/jase.202308\\_26\(8\).0011](http://dx.doi.org/10.6180/jase.202308_26(8).0011)

## Highlights

- Neem biodiesel physico-chemical properties were determined in compliance with international biodiesel standards.
- Improvement in cold flow properties (CP, PP, and CFPP) of neem biodiesel by adding kerosene and mineral diesel.
- Neem biodiesel mixed with petroleum-derived fuels

(B20\*\*) and natural turpentine oil (B10T10) showed comparable cold flow qualities with mineral diesel.

- Due to their high volatility rate, the cold flow characteristics of biodiesel blends did not showed improvement with diethyl ether and n-butanol.
- The positive net energy balance of Neem biodiesel produced was found as 14.28%.

## 1. Introduction

The pace of a country's socio-economic development and environmental sustainability is determined by its energy security. On the other hand, rapid industrialization and urbanization raise energy demand, resulting in the depletion of petroleum crude oil reserves. Similarly, the intensive use of fossil fuels to meet energy needs contributes to carbon emissions, which causes climate change and global warming [1, 2]. The depletion of petroleum crude oil reserves and the increasing greenhouse gas emissions caused by petroleum-based fossil fuels have prompted a search for alternative energy sources that are less harmful to the environment [3–5]. Alternative liquid biofuel (such as biodiesel) is environment-friendly promising fuel with better combustion properties with respect to conventional petroleum-based fossil fuels containing oxygen 10% by weight and having no aromatics content [2]. Biodiesel is regarded as one of the most competitive alternative fuels to mineral diesel, with more significant cetane numbers, lower emissions of unburned hydrocarbons, particulate matter, and carbon monoxide, and insignificant sulfur dioxide emissions after combustion in compression ignition engines [6, 7]. However, it produces more CO<sub>2</sub> due to its better combustion properties, thus making it eco-friendly and suitable alternative fuel [8, 9].

The studies conducted in the past on the production of biodiesel from natural resources such as palm oil [10], castor oil [11], used vegetable oil [12], frying oil [13], microalgae [14], Argemone seed oil [15], seed oil from Chinese tallow [16], *Jatropha Curcas*, etc. [13] but its inferior cold flow properties make hindrance in its utilization in cold weather conditions.

The cold flow behaviour of biodiesel is measured with cloud point (CP), pour point (PP), cold filter plugging point (CFPP), and filterability test at low temperatures. Biodiesel's unacceptable cold flow behaviour is responsible for gumming fuel, which obstructs filters, leading to poor engine performance and causing ignition problems in cold weather conditions. The ignition problem results in partial combustion of fuel, leading to deteriorating engine starting operation [8]. The usage of biodiesel at low temperatures

induces the production of solid wax crystal nuclei, which grow in size as the temperature is further reduced. The nuclei of solid wax crystals become more apparent at this temperature, known as cloud point (CP). The crystal nuclei aggrandize further below this temperature range, preventing unrestricted fluid pouring; this temperature is referred to as the pour point (PP) [17].

While the cold filter plugging point (CFPP) is the lowest temperature at which fuel flows freely through the fuel injection system in a specific amount of time. The poor flow properties of biodiesel cause the formation of crystals in fuel particles, and improvement can be made by applying different techniques such as winterization, blending, and adding additives. Different studies have been conducted to make the flow properties of biodiesel acceptable for engine operation. Winterization was found as an effective method to boost the flow behaviour of biodiesel but simultaneously reduces its oxidation stability with a deficiency of saturated fatty acids [13]. A variety of chemical additives, such as commercial PAM (poly-alkyl methacrylate) co-polymer, were used to improve the cold flow properties [10]. Another study looked at the impact of surfactants such as sugar esters (S270 and S1570), silicone oil (TSA750S), polyglycerol ester, and diesel additives on improving the cold filter plugging point of waste cooking oil biodiesel. The use of long-chain alcohols with transesterification and fractional crystallization were two other strategies examined to improve biodiesel's low-temperature flow properties with diesel mixing [8].

Blending is an effective method for improving in low-temperature flow properties of biodiesel without any effect on its yield [13]. As a result, diesel, kerosene, and ethanol are the most commonly employed cold flow enhancers in the blending techniques. A previous study found that a B20 blend including kerosene and mineral diesel mixture significantly impacts low-temperature flow qualities. Diesel blending boosts CP and PP by 57.61% and 78.57%, respectively, whereas kerosene boosts CP and PP by 62.94% and 85.78%. While adding 20% more ethanol improved CP and PP by 60.48% and 63.96%, utilizing 20% more ethanol significantly influenced cold flows [1].

The addition of branched-chain fatty acid methyl esters (BC-FAME) can be used as additives (e.g., methyl iso-oleate and methyl iso-stearate) and diluents to reduce the CP and PP of biodiesel. The saturated branched chain-FAME (Me iso-C18:0) showed a better effect than that of unsaturated branched chain-FAME (Me iso-C18:1) to improve the cold flow property of the palm oil methyl ester, castor oil methyl ester, and soy methyl ester when used as additives (up to 2%). A similar trend of effectiveness was also

reported when these BC-FAMES were used as diluents. Up to 50% mix of Me-iso-C18:0 as a diluent reduced the CP and PP of palm oil methyl ester, castor oil methyl ester, and soy methyl ester up to acceptable ranges. Moreover, other branched-chain esters, e.g., isopropyl as well as 2-butyl esters of fats and oils, typically have better low-temperature flow properties than their corresponding straight-chain isomers. It was observed that saturated FAMES with a higher melting point deteriorate the cold flow properties. The saturated FAMES can be reduced by blended *Citrus colocythis* oil biodiesel and *Camelus dromedaries* fat biodiesel. Both blends reduced the saturated FAMES, and as a result, there was a significant improvement in cold flow properties was observed [18].

Furthermore, the addition of cold flow improvers such as bioethanol blending with diesel and winterization boosts the cold flow properties of *Pongamia pinnata* biodiesel. Winterization lowers the CP and PP of biodiesel by 5 °C, while introducing diesel blending in biodiesel reduces the CP by 9 °C and PP by 11 °C. In contrast, kerosene blending brings down the CP to 11.5 °C and PP by 12.5 °C [19].

Previous research analysis on engine performance and emission testing on various biodiesel-kerosene blends found that brake thermal efficiency increases as kerosene concentration in biodiesel blends are increased. At the same time, brake specific fuel consumption increases with high concentrations of biodiesel due to their lower heat content but decreases as kerosene concentration increases in blends. With increased kerosene concentrations, carbon monoxide (CO) and hydrocarbons (HC) emissions were produced due to incomplete combustion, but they decreased with increasing biodiesel concentrations. In addition, nitrogen oxides (NOx) emissions were reduced by 10 to 18% in a 15% biodiesel blend compared to a 60% biodiesel blend as the increased kerosene [20]. Therefore, when biodiesel fuel blends with kerosene and diesel are used in an engine, no negative impact on engine performance is found.

Diesel blends containing biodiesel, ethanol, and butanol were produced in order to analyze the combustion, performance, and exhaust emission of common rail direct injection (CRDI) diesel engine. Biodiesel was produced through single stage transesterification process, and then blends of Biodiesel (B40), and Biodiesel-ethanol-butanol (B40 E10 BUT10) were tested at two different injection pressures (300 and 600 bar) against mineral diesel fuel. The experimental results show that thermal efficiency in diesel fuel was higher than in biodiesel blends. Carbon dioxide (CO<sub>2</sub>) emission is low in the biodiesel blend of (B40 E10 BUT10) at 300 bars due to the presence of fewer carbon atoms in the blend. The oxides of nitrogen (NOx) emission

were found decreasing in B40 at 300 bars. The CRDI engine was tested for various fuel injection pressures using B40 E10 BUT10. The brake thermal efficiency of biodiesel blends was found to be slightly lower than mineral diesel fuel. Comparing blends for NOx emissions, the B40 blend at 300 bars with increasing load, having proper combustion, resulted in fewer emissions, even lower than diesel fuel. The performance of the HC emission showed that B40 at 300 bar pressure emits less than the diesel fuel. Similarly, comparing the CO<sub>2</sub> emission, the blend (B40 E10 BUT10) at 300 bar emits less CO<sub>2</sub> than the diesel fuel. Therefore, these results demonstrate that the prepared biodiesel blends have lower emissions and slightly increased efficiency. The engine knocking problem was also reduced by using blended biodiesel with butanol which lowers the calorific value and thus improves the knocking sounds, but it is also discovered that it is helpful in lowering emissions and helps complete combustion [21].

Turpentine oil (a natural organic solvent) was employed as a blending agent with *Jatropha curcas* biodiesel in a previous study, and the engine performance was examined. Turpentine oil has a higher calorific value and lower kinematic viscosity than biodiesel made from *Jatropha curcas* oil, allowing for complete combustion of the fuel. Turpentine oil blends also emit less CO, HC, particulates, and NOx, with 13.04%, 17.5%, 30.8%, and 4.21%, respectively [22]. Previous experimental results on engine performance and emission characteristics of different blends of *Jatropha*-Mineral Turpentine oil as fuel indicated that brake thermal efficiency of the blend of 80% *Jatropha curcas* biodiesel and 20% of mineral turpentine was comparable to diesel fuel. Carbon monoxides (CO) and hydrocarbon (HC) emissions were reduced to a considerable amount, whereas the oxides of nitrogen (NOx) increased with an increase in engine load operations. The specific fuel consumption of *Jatropha*-Mineral Turpentine blends was slightly higher than diesel fuel. *Jatropha*-Mineral Turpentine blends' heat release rate and cylinder pressure were closer to that of diesel fuel. The engine test results indicated that *Jatropha*-Mineral Turpentine oil blends might be used in a traditional compression ignition engine without any modification [23].

Another study used diethyl ether to improve the engine performance and emission attributes of Neem methyl ester (biodiesel). The peak pressure in the cylinder and heat flow rate for BD5 (5% by volume diethyl ether mixture) were somewhat more significant than other fuel blends and B100 in engine testing. Biodiesel blending with 5% diethyl ether showed improvement in brake-specific fuel consumption and thermal efficiency. Compared to other blended fuels and B100, smoke and CO emissions from

5% blended biodiesel was found to be reduced. Due to the higher temperature of exhaust gases after biodiesel combustion, NO<sub>x</sub> emissions were higher for 5% blended biodiesel fuel than mineral diesel. Unburned hydrocarbon emissions were higher for all biodiesel and diethyl ether blends with respect to biodiesel blends at all loads. Therefore, it was observed that adding 5% by volume of diethyl ether in biodiesel can effectively reduce emissions of toxic gases from diesel engines without requiring major internal changes in an engine [24].

Past research investigations on low-temperature flow and filterability properties of n-butanol and ethanol blends with diesel and biodiesel fuels showed that n-butanol blends have better cold flow properties than ethanol blends due to their better homogenous mixing property because intermediate alcohol content in ethanol-diesel blends have weak homogenous mixing property. Biodiesel fuel acts as a stabilizing component because strong interactions occur between the alcohol and the ester group's hydroxyl group. Despite the fact that the CFPP of heavier alcohols is usually higher for higher alcohol contents, no significant differences in CFPP were observed between different alcohols blended up to B40. Interestingly, the addition of higher long carbon-chain alcohols reduced CFPP values [25].

The non-edible Neem (*Azadirachta indica*) vegetable oil seed is widely available and native to the Indian sub-continent and most African countries. In the future, this feedstock could be utilized to produce biodiesel. The annual production of Neem oil seeds per plant is estimated to be between 30 and 50 kgs, with an oil content yield of about 40% by weight, making it a possible biodiesel source. Similarly, Neem seed oil contains a higher amount of triterpenoid compounds and triglycerides, as well as significant saturated fatty acids (such as palmitic and stearic acid) and polyunsaturated fatty acids (such as oleic and linoleic acids), making it suitable for biodiesel fuel production [26, 27].

**Motivation and objective:** This study aimed to investigate into the combination of petroleum-derived products (such as kerosene, mineral diesel, and mixed kerosene/diesel) and natural organic components (such as turpentine oil, diethyl ether, and n-butanol), which can affect the cold flow qualities of *Azadirachta indica* (Neem) biodiesel. As a result, the measured physicochemical and cold flow parameters of various biodiesel fuel blends were compared. FTIR (Fourier-transform infrared spectroscopy) investigations were used to distinguish various fuel blends by identifying discrete spectral signatures. The cost-effectiveness of blending Neem biodiesel with kerosene, mineral diesel, mixed kerosene/diesel, and turpentine oil as cold flow improvers

were assessed and compared.

## 2. Materials and method

Neem oil was extracted from local seeds using a cold-pressed mechanical expeller. The mineral diesel utilized in this investigation was obtained from a company-operated gasoline station of Pakistan State Oil (PSO). Kerosene oil (Lucky Oil Company Ltd, Pakistan), turpentine oil (Vietnam Gum Rosin Processing, Vietnam), diethyl ether (Merck, Germany), and n-butanol (Merck, Germany) were procured from the market. All experiments were carried out in the Biodiesel Laboratory of the Department of Environmental Engineering, NED University of Engineering and Technology, Karachi, at a room temperature of 28 ± 1 °C.

### 2.1. Acid value measurement

The acid value test was used to determine the fatty acid content of Neem oil before proceeding with the transesterification procedure. 1 g of Neem oil was mixed with 100 mL of ethyl alcohol (Analytical grade, Merck, Germany) in a 250 mL flask to calculate the acid value. Two drops of phenolphthalein were used as an indicator for titration. The flask was then heated in a water bath (Thermostat Waterbath HH6, Wincom Company Ltd, China) for 10 min at 65°C with constant stirring before being cooled to room temperature. The solution was titrated against 0.1 N KOH until a light pink color appeared, indicating the reaction's endpoint. The following mathematical expression was used to compute the acid value (AV) based on the titration readings.

$$\text{Acidvalue} = \frac{56.1VN}{W} \quad (1)$$

Where V is the amount of standard solution of potassium hydroxide used in mL, N is the normality of the potassium hydroxide, and W is the mass of Neem oil sample (g).

### 2.2. Two steps acid-base catalyzed transesterification reaction

The protocol for this reaction includes acid esterification followed by base transesterification as per literature [28]. Fig. 1 presents the schematic illustration of biodiesel production from Neem oil. Non-edible Neem oil (40 g) was weighed using an analytical balance (AB 304-S, Mettler Toledo, Switzerland), and then it was heated at 100 °C with continuous stirring for about 30 min to reduce its viscosity and moisture content in a 500 mL flask placed on hot plate stirrer MS-20A, Daihan Scientific Company, South Korea. Then the temperature was brought down to 50 °C for acid-catalyzed esterification, and heated oil was reacted with 24

g of methanol, i.e. (5:3 w/w) utilizing concentrated sulfuric acid (Analytical Grade, Merck, Germany) in a 500 mL flask connected with a fractional column and condenser assembly to reflux evaporated methanol during the reaction. The reaction mixture was continuously heated at 50 °C and stirred for 1 hour at a mixing speed of 300 rpm. The mixture was allowed to cool down slowly for 2 hours after the first reaction to help evaporate water content produced and remove mixture impurities by sedimentation at room temperature.

In the second step, transesterification with base catalyst, 8 g of methanol, and 0.64 g NaOH was added to the product of acid-catalyzed esterification. The whole mixture was heated to 65 °C for 2 hours with a continuous stirring speed of 300 rpm. Soon after completion of the base transesterification reaction, the mixture was left undisturbed to settle down under the action of gravity for at least 24 hours in a 1 L capacity separating funnel to get two distinct layers of biodiesel (fatty acid methyl ester) and glycerol as a byproduct of the reaction. These layers formed due to the difference in densities between biodiesel and glycerol, causing biodiesel to rise to the top and glycerol to settle at the bottom. Decantation was used to separate the biodiesel from the crude glycerine. Next, a water wash of biodiesel was carried out using warm de-ionized water at 50 °C to remove contaminants, followed by drying in an oven at 100 °C for 1 hour. Gravimetric analysis was used to determine the amount of biodiesel and glycerol being produced.

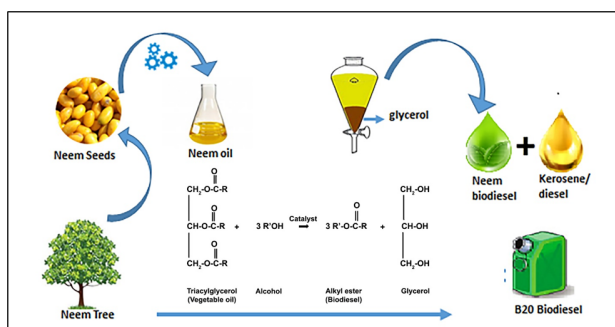


Fig. 1. Scheme for the synthesis of biodiesel from Neem seeds.

### 2.3. Physicochemical characterization of Neem biodiesel

The density of raw Neem oil and biodiesel product was determined as per ASTM D1298 by density meter (D130N, Kem Kyoto Electronics, Japan). The density of the measured sample was divided by the corresponding density of water (0.997 g/mL) at a room temperature of 28 °C to determine the specific gravity of the samples.

**Kinematic viscosity:** Kinematic viscosities of extracted

Neem oil and biodiesel produced were measured using Kinematic/ Dynamic viscometer (VDM-300, AS Lemis, EU) following ASTM D445.

### Cloud point (CP) and pour point (PP) measurement:

Cloud point (CP) and pour point (PP) were measured by Cloud / Pour Point Tester (MPC-102L, Tanaka, Japan) as per ASTM D2500 and ASTM D97, respectively.

**Cold filter plugging point (CFPP):** Cold Filter Plugging Point was measured by a CFPP tester (AFP-102, Tanaka, Japan) following ASTM D6371.

**Cetane number index:** Cetane number was calculated by measuring the aniline point temperature (°C) using Aniline Point Tester (Koehler Instrument Company Inc, USA). API gravity was calculated using the following formula.

$$API\ gravity = \frac{14.5}{specific\ gravity} - 131.5 \quad (2)$$

After calculating the API gravity and measured aniline temperature, the diesel index was calculated, and then finally cetane number was calculated by using the following mathematical expressions:

$$Diesel\ Index = Aniline\ point(^{\circ}C) \times \frac{API\ gravity}{100} \quad (3)$$

$$Cetane\ Number = Diesel\ Index - 3 \quad (4)$$

**Calorific value test:** Calorific values of extracted Neem oil and blended biodiesel fuel samples were measured with an oxygen bomb calorimeter (IKA C200, Germany) according to the ASTM D240 standard method.

**Flash Point test:** Flashpoint (°C) of prepared fuel blended samples were measured with a flashpoint tester (SCAVINI, Italy) following the ASTM D93 standard method.

**Refractive:** Refractive indexes of blended samples were measured with (Abbe-2WAJ Refractometer, China) at the Department of Polymer and Petrochemical Engineering, NED University, Karachi.

### 2.4. Sample preparation (blending biodiesel with kerosene, diesel, the mixture of kerosene/ diesel, turpentine oil (TP), diethyl ether (DEE), and n-butanol)

The binary and ternary blending ratios by volume % of Neem biodiesel with kerosene, diesel, the mixture of kerosene/diesel samples was prepared following literatures [29, 30] and are presented in Table 1. Whereas Neem biodiesel blends (10% and 20%) were prepared with turpentine oil (TP), diethyl ether (DEE), and n-butanol in percentage volume of 5% and 10%, along with the remaining volume topped up with mineral diesel to make of 100 mL (see Table 2).

**Table 1.** Fuel composition blending ratios of Neem biodiesel with kerosene, diesel, and mixture of kerosene- diesel (by volume %).

Fuel blends	Biodiesel: Kerosene	Fuel blends	Biodiesel: Diesel	Fuel blends	Biodiesel: Kerosene: Diesel
B0	0:100	B0*	0:100	B0**	0:50:50
B20	20: 80	B20*	20: 80	B20**	20:40:40
B40	40:60	B40*	40:60	B40**	40:30:30
B60	60:40	B60*	60:40	B60**	60:20:20
B80	80:20	B80*	80:20	B80**	80:10:10
B100	100:0	B100*	100:0	B100**	100:0:0

\*Blended biodiesel with mineral diesel

\*\*Blended biodiesel with kerosene and mineral diesel

**Table 2.** Fuel composition blending ratios of Neem biodiesel with turpentine oil, diethyl ether, and n-butanol (by volume %).

Fuel blends	Biodiesel: Diesel: Turpentine oil	Fuel blends	Biodiesel: Diesel: Diethyl ether	Fuel blends	Biodiesel: Diesel: n-butanol
B10T5	10:85:05	B10EE5	10:85:05	B10BU5	10:85:05
B10T10	10:80:10	B10EE10	10:80:10	B10BU10	10:80:10
B20T5	20:75:05	B20EE5	20:75:05	B20BU5	20:75:05
B20T10	20:70:10	B20EE10	20:70:10	B20BU10	20:70:10

**Composition of fatty acids:** Profile of fatty acids composition of Neem biodiesel was obtained by GC-FID (Gas chromatography flame ionization detector, Shimadzu 2010, Japan) equipped with Capillary GC Column SP-2560 (100 m × 0.25 mm × 0.20 μm) at Pakistan Council for Scientific and Industrial Research (PCSIR) Laboratories, Karachi, Pakistan.

**FTIR analysis of Neem biodiesel:** A Thermo Fisher Scientific Nicolet IS10 Fourier transform infrared (FTIR, Waltham, USA) in attenuated total reflection mode (ATR) having ZnSe crystal sampling accessory used for acquiring Fourier transform infrared (FTIR) spectra of biodiesel, kerosene, diesel, turpentine oil (TP), diethyl ether (DEE) and n-butanol blends in the range of 600-3500cm<sup>-1</sup>. Two replicates from each sample were analyzed by averaging 16 scans per sample at a resolution of 4 cm<sup>-1</sup> at room temperature (28 ± 1 °C). FTIR tests were conducted at the Department of Chemistry, NED University, Karachi.

## 2.5. Cost estimation of Neem biodiesel production

The cost analysis of 1 L biodiesel production from Neem oilseed was calculated. Raw Neem oil cost was Rs.100/L, while the esterification and transesterification costs were calculated based on the consumed amount of methanol, sulphuric acid (H<sub>2</sub>SO<sub>4</sub>), and sodium hydroxide (NaOH) multiplied by their respective market values. The heating and mixing (stirring) utilities charges were calculated by multiplying the power consumption of equipment (0.650 kW) by its total operating time for both esterification/transesterification processes (3.5 hours) and the area fraction of the equipment [i.e., container base area (38.46

cm<sup>2</sup>)/Heating element base area (324 cm<sup>2</sup>) = 0.1187] as per literature [31] and further multiplied with electric tariff charges (Rs.15/ kWh) of local electricity provider [32]. The revenue generated from glycerol as a byproduct (10% produced by volume) and the methanol recovery cost (70% by volume of its total consumption) were calculated by multiplying their respective unit market price. The difference in the total biodiesel input production cost and generated revenue gives the net cost of biodiesel production in Pak Rupees per liter (USD/L). Furthermore, the costs of blended biodiesel with kerosene (B20), mineral diesel (B20\*), mixed kerosene/diesel (B20\*\*), and turpentine oil (B20T10) were calculated based on the market price of kerosene PKR 109.53 per L, mineral diesel PKR 137.62 per L, and turpentine oil PKR 200 per L [33].

## 2.6. Energy balance of biodiesel production

The input energy of Neem biodiesel production using the heating and stirring was calculated as 2.275 kWh (8.190 MJ) by multiplying the power consumption of equipment with operating time (3.5 hours) and area fraction (0.1187). At the same time, the methanol consumption energy input was calculated by assuming 70% methanol recycled through distillation assembly. Therefore, 0.07 L was multiplied by its density of 0.79 kg/L and calorific value (22.7 MJ/kg). The energy input consumption of H<sub>2</sub>SO<sub>4</sub> and NaOH used in production was considered negligible. The energy output was calculated by multiplying the mass of biodiesel and glycerol produced in kgs with their respective calorific values. The energy balance (energy efficiency) was obtained by dividing the energy output by the energy input required

for biodiesel production.

### 2.7. Statistical analysis

The mathematical regression model equations were obtained to predict the influence of different cold flow improvers such as kerosene, diesel, and mixture of kerosene/diesel on low-temperature flow patterns of varying fuel blends. Linear equations were developed with a regression coefficient of determination ( $R^2$ ) with a 95% confidence level by using Microsoft Excel Software (2013).

## 3. Result and discussion

### 3.1. Biodiesel and glycerol yield

Fatty acids present in vegetable seed oils (saturated and unsaturated) have an influence on the cold flow pattern and oxidation stability of Neem biodiesel. It is interesting to note that both properties oppose each other. According to the previous literature, if the vegetable seed oil has an acid value higher than 4 mg potassium hydroxide per g of vegetable oil, then a single *transesterification* reaction is not recommended because it makes soap formation. Therefore, the acid value of vegetable seed oil (free fatty acid content) needs to be measured before reacting with alcohol to produce biodiesel [19]. The acid value of Neem oil was calculated as 31.5 mg KOH per g of Neem oil, i.e., much higher than the standard value for direct *transesterification* of vegetable seed oil. Thus, two-step *transesterification* processes were opted to produce Neem biodiesel. The biodiesel and glycerol yields were measured as  $27.49 \pm 1.52$  g / 40 g oil (68.72% by weight) and  $12.50 \pm 1.78$  g/40 g oil (% by weight), respectively (results are presented as mean  $\pm$  SD for sample size = 3).

### 3.2. Characterization of Neem oil, Neem biodiesel, and blended samples

The measured physical and chemical properties of Neem oil and biodiesel are presented in Table 3. The characterization of Neem biodiesel was found in accordance with international biodiesel standards ASTM D 6751 and EN 14214. Physico-chemical properties of blended samples with petroleum products (kerosene, mineral diesel, and mixed kerosene/ diesel) were measured and depicted in Table 4. It was noted that by increasing biodiesel concentration in blends, the values of density, kinematic viscosity, and flash point were also increased with kerosene, diesel, and mixed kerosene/ diesel. It was in accordance with previous literature [34]. Blended biodiesel fuels showed flash points higher than kerosene oil and diesel, ensuring safe handling and storage.

Moreover, reducing the concentration of biodiesel in the blended samples improved its calorific values; this, in fact, was due to biodiesel's low calorific value in contrast to kerosene (42 MJ/kg) and mineral diesel (46 MJ/kg). However, the calorific value was reduced to about 11.12% for B20 blended fuel compared to mineral diesel due to blending [35]. The results showed that increasing the concentration of biodiesel in the blends with kerosene and mineral diesel reduced its cetane number. B20\*\* sample showed the highest flash point (80 °C) and calorific value (45.33 MJ/kg).

Table 5 shows the physicochemical parameters of biodiesel blended fuel samples with natural organic compounds. Increasing the proportion of turpentine oil in fuel blends with B10 and B20 reduces the kinematic viscosity, flash point, and refractive index while increasing the calorific value. According to the previous literature, when the proportion of diesel fuel in fuel blends is increased, the flashpoint and kinematic viscosity values reduce, while the refractive index value increases [36]. However, in this current investigation, results noticed that turpentine oil influences the fuel blends properties such as it enhances calorific value but lowers kinematic viscosity, flash point, and refractive index with an increasing percentage in blends from 5% to 10%. Because the kinematic viscosity of pure turpentine oil is 1.2 mm<sup>2</sup>/s and calorific value is 46.63 MJ/kg, which helps in further reduction in the kinematic viscosity and enhancement in the calorific value of biodiesel blends. The flashpoint of biodiesel blended with natural turpentine oil (B10T10) was 67 °C, and its calorific value was measured as 49.58 MJ/kg. The increasing volume % of diethyl ether and *n-butanol* with B10 and B20 fuel blends reduces their kinematic viscosity, calorific value, flash point, and refractive index. Adding more turpentine oil, diethyl ether, and *n-butanol* to fuel blends reduces their kinematic viscosity and related refractive indices, indicating that light beam travels quicker across the medium of samples. The disadvantage of blending biodiesel with diethyl ether and *n-butanol* is that they have higher latent heats of vaporization, i.e., 350 kJ/kg and 585 kJ/kg, respectively than turpentine oil. The latent heat of vaporization of turpentine oil is 293 kJ/kg, making it more suitable for biodiesel blending.

### 3.3. Composition of fatty acids

Compared to other fatty acids, the analysis of the fatty acid composition of Neem oil revealed the presence of palmitic acid, stearic acid, stearic acid, oleic acid, and linoleic acids in higher concentrations, as depicted in Table 6. It was also endorsed by researchers in their studies that Neem oil contains four significant fatty acids, i.e., saturated fatty

**Table 3.** Physical and chemical properties of raw Neem oil and its biodiesel.

Properties	Neem oil	Neem biodiesel	ASTM D 6751
Density (g/mL)	0.917	0.877	0.86 - 0.90*
Specific gravity @ 28 °C	0.919	0.879	-
Kinematic viscosity (mm <sup>2</sup> /sec)	29.37	5.22	1.9 - 6.0
Calorific value (MJ/kg)	41.12	39.37	-
Flashpoint (°C)	280	170	130 minimum
Cetane number	-	47.20	47 Minimum

\*EN 14214 (European Biodiesel Standard)

**Table 4.** Physico-chemical properties of biodiesel blends prepared with kerosene and mineral diesel.

Fuel blends	Density (g/cm <sup>3</sup> )	Specific gravity	Kinematic viscosity (mm <sup>2</sup> /sec)	Calorific value (MJ/Kg)	Flash point(°C)	Refractive Index
Blended biodiesel with kerosene						
B0	0.777	0.779	2.71	48.79	43	1.3910
B20	0.795	0.797	3.17	47.43	50	1.4455
B40	0.817	0.819	3.75	45.23	62	1.4475
B60	0.839	0.814	4.25	44.72	68	1.4495
B80	0.859	0.861	4.92	43.73	75	1.4535
B100	0.877	0.879	5.22	39.37	170	1.4585
Blended biodiesel with mineral diesel						
B0*	0.822	0.824	4.43	45.11	61	1.4320
B20*	0.831	0.833	4.64	44.30	76	1.4544
B40*	0.843	0.845	4.85	42.61	78	1.4562
B60*	0.854	0.856	4.99	41.35	80	1.4572
B80*	0.866	0.868	5.14	40.85	88	1.4595
Blended biodiesel with mixed kerosene and mineral diesel						
B0**	0.800	0.803	1.66	51.71	46	1.4555
B20**	0.810	0.813	2.75	49.58	67	1.4558
B40**	0.828	0.831	3.76	45.02	78	1.4565
B60**	0.847	0.851	4.03	44.72	85	1.4569
B80**	0.865	0.871	4.82	41.39	90	1.4570

\*Blended biodiesel with mineral diesel

\*\*Blended biodiesel with kerosene and mineral diesel

acid such as palmitic acid and stearic acid; polyunsaturated fatty acids such as oleic acid and linoleic acids [26]. Past studies observed that it is not necessary for the occurrence of low content of saturated fatty acids with respect to unsaturated fatty acids in biodiesel will have acceptable cold flow properties. Fatty acid composition of different vegetable oil feedstocks depends on the origin of oil, oil extraction techniques and its quality. The GC analysis of Neem oil showed that the total percentage of unsaturated fatty acid was 66.38%, while the percentage of saturated fatty acid was 33.54%. It was observed that biodiesel containing higher unsaturated fatty acids has higher density and calorific value but has lower kinematic viscosity and cetane number. Moreover, biodiesel produced from highly saturated fatty acids has lower thermal efficiency and emits less unburned hydrocarbons, carbon monoxide, and smoke [1].

### 3.4. Effect of blending on Neem biodiesel cold flow properties

In general, B20 and lower-level biodiesel blends with conventional diesel can be used without modification in CI engines. Therefore, the effects of blending Neem biodiesel 20% by volume with petroleum-derived products (kerosene oil, mineral diesel, and a mixture of kerosene/diesel) and natural organic solvents (turpentine oil, diethyl ether, and n-butanol) on cold flow properties were measured and discussed below.

#### 3.4.1. Cloud Point (CP)

Fig. 2 depicts the cloud point measured of biodiesel blending with kerosene, mineral diesel, and mixed kerosene/diesel. Increasing the blending ratio of kerosene by % volume reduced the CP from 12 °C with B100 to -10 °C with B20 blend. The regression analysis showed an R squared value for CP ( $R^2=0.958$ ) obtained. The experiment results are highly significant with respect to the linear regression



**Table 5.** Physico-chemical properties of biodiesel blends prepared with kerosene and mineral diesel.

Blended biodiesel with mineral diesel and turpentine oil (BD+D+TP) in % volume									
Fuel blends	Density (g/cm <sup>3</sup> )	Specific gravity	Kinematic viscosity (mm <sup>2</sup> /sec)	Calorific value (MJ/Kg)	Flash point (°C)	Refractive Index	CFPP (°C)	CP (°C)	PP (°C)
B10T5	0.828	0.830	2.85	44.57	84	1.4650	6	5	-2
B10T10	0.832	0.834	2.84	45.33	80	1.4645	7	5	-3
B20T5	0.836	0.838	2.93	44.00	90	1.4655	8	6	-1
B20T10	0.839	0.841	2.88	44.24	88	1.4650	7	5	-2
Blended biodiesel with mineral diesel and diethyl ether (BD+D+DEE) in % volume									
B10EE5	0.820	0.822	1.72	43.96	50	1.4570	7	4	-3
B10EE10	0.813	0.815	1.58	43.40	46	1.4660	4	2	-5
B20EE5	0.827	0.829	2.36	43.39	64	1.4630	5	3	-4
B20EE10	0.822	0.824	1.77	42.83	58	1.4620	3	-1	-6
Blended biodiesel with mineral diesel and n-butanol (BD+D+BU) in % volume									
B10BU5	0.813	0.815	2.34	43.89	82	1.4665	2	-2	-5
B10BU10	0.812	0.814	2.19	43.26	74	1.4660	1	-4	-6
B20BU5	0.828	0.830	3.27	43.83	70	1.4520	7	5	0
B20BU10	0.825	0.827	2.54	43.70	64	1.4460	6	3	-1

**Table 6.** Fatty Acid Composition of Neem Oil.

Name of fatty acid	% Composition
Myristic acid (C14:0)	0.01
Palmitic acid (C16:0)	15.62
Palmitoleic acid (C16:1)	Traces
Stearic acid (C18:0)	16.71
Oleic acid (C18:1)	50.60
Linoleic acid (C18:2)	15.18
Arachidic acid (C20:0)	1.20
Linolenic acid (C18:3)	0.60
Cis-11-eicosenoic acid (C20:1)	Traces

best fit model with an empirical equation as  $y = -4.971x + 14.733$ . Reasonable CP result of Neem biodiesel (B20\*) was found to be reduced with a blending ratio of 80 % mineral diesel to 8 °C from 12 °C. Statistically significant value  $R^2=0.954$  was obtained from the experimental data, showing linear trends with equation;  $y = -0.914x + 12.367$ . Similarly, CP was improved from 12 °C to -4.5 °C using a B20\*\* blend with mixed kerosene and diesel. The regression equation was  $y = -4.042x + 14.4$  with coefficient of regression (0.973). Similar trends of measured values were reported in literatures [2, 3] related to the cloud point (CP) of *Moringa oleifera* biodiesel blends with mineral diesel.

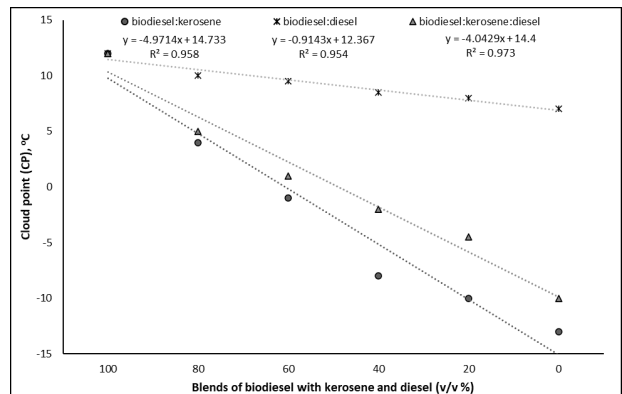


**Fig. 2.** Effect of Neem biodiesel ratio on CP of biodiesel:kerosene, biodiesel: diesel and biodiesel:kerosene:diesel blends.

Table 5 shows the effect of natural organic solvents on the cold flow characteristics of Neem biodiesel. The CP temperature was enhanced by adding turpentine oil, diethyl ether, and n-butanol to fuel blends at a 5 to 10% concentration by volume. However, turpentine oil blends with biodiesel and diesel than diethyl ether and n-butanol are recommended because they have a higher latent heat of vaporization, which have a very low latent heat vaporization, causing the solvents to evaporate more quickly even at room temperature. As a result, comparing the effects of

combining biodiesel with mineral diesel and turpentine oil, the B20T10 blend was found to have improved cold flow qualities such as CP being reduced from 12 °C to 5 °C, and physicochemical properties are comparable to international biodiesel standard.

### 3.4.2. Pour Point (PP)

The impact of blending biodiesel with kerosene, mineral diesel, and mixed kerosene/diesel on pour point (PP) was measured and presented in Fig. 3. Improvement in PP was achieved at B20 having 20 % by volume Neem biodiesel blended with 80 % kerosene dropped from 10 °C to -19 °C. The R squared value was found to be 0.985, which showed that the experiment results were significant, and an empirical linear equation was developed as;  $y = -6.485x + 14.867$ . It was noticed that kerosene has a better impact on the improvement of blended biodiesel cold flow properties as compared to mineral diesel [1]. Similarly, the PP value of Neem biodiesel was reduced from 10 °C to 2 °C for blending ratio with 80% mineral diesel (B20\*). The plot between the % Neem biodiesel with respect to the PP showed  $R^2=0.989$  and has a linear equation as  $y = -1.814x + 11.433$ . According to previous literature, the maximum blending ratio with the addition of 20 % biodiesel is suggested for its utilization as an alternative fuel under cold climatic conditions without causing any adverse effect on the engine performance [4, 20]. Therefore, the B20\*\* blend with mixed kerosene and diesel improved the PP from 10 °C to -7 °C. It was observed in the previous literature that PP was improved by blending biodiesel with a mixture of kerosene and diesel [19]. The regression model equations for PP are presented as  $y = -4.871x + 14.967$ , with  $R^2 = 0.965$ . It was noticed that kerosene has a better impact on the enhancement of the cold flow pattern of blended biodiesel comparing to mineral diesel [1]. Therefore, an equal mixture of kerosene and diesel addition in biodiesel blends (B20\*\*) has a significantly better impact on its cold flow properties. Although the CP and PP of a blend of Neem biodiesel and kerosene are lower than a blend of Neem biodiesel and diesel, it is recommended to use a mixture of kerosene and mineral diesel rather than pure kerosene oil for safe operation in any CI engine which is designed to run on petroleum diesel.

The addition of 5% and 10% of turpentine oil, diethyl ether, and n-butanol with biodiesel blends showed limited influence on the enhancement in CFPP, PP, and CP by approximately 1 °C as presented in Table 5. However, a natural turpentine oil blend (B20T10) is more preferred in cold weather conditions as compared to diethyl ether and n-butanol due to its higher flash point and calorific value, making the fuel blend more favorable for its use in the

diesel engines.

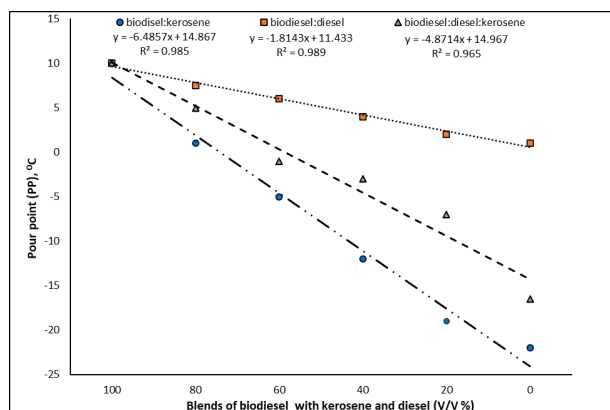


**Fig. 3.** Effect of Neem biodiesel ratio on PP of biodiesel: kerosene, biodiesel: diesel and biodiesel:kerosene:diesel blends.

### 3.4.3. Cold Filter Plugging Point (CFPP)

Cold filter plugging points are measured with respect to different blends and shown in Fig. 4. Improvement in the CFPP with an increasing ratio of biodiesel in kerosene blend (B20) was most prominent. The previous study observed a similar trend of reducing CFPP temperature by increasing kerosene blending by 80% by volume [29]. B20 results showed that CFPP improved from 15 °C with B100 to -20 °C. The regression value of  $R^2=0.926$  showed that the experimental results are significant between Neem biodiesel and kerosene, with regression correlation obtained for CFPP ( $y = -10.514x + 30.467$ ). The cold flow characteristics of Neem biodiesel were evaluated when blended with mineral diesel (B20\*). The findings showed that the CFPP of blended biodiesel with diesel was improved to 6 °C from 15 °C of biodiesel (B100) measured value. Neem biodiesel (B100) CFPP is not good enough for cold flow properties as fuel during the winter conditions. Therefore, it can be mentioned that by increasing the diesel ratio in fuel blends, the CFPP decreases, making it useful for its applications in cold weather. CFPP of B20\* blended fuel linear regression  $R^2$  value was found to be 0.970 with an empirical equation as  $y = -2.142x + 17.333$ . The results showed a linear trend in CFPP improvement as per the profile obtained after experimental measurements in accordance with past studies [3, 4]. CFPP of blended biodiesel with mixed kerosene and diesel (B20\*\*) showed an improvement from 15 °C to -8 °C. Linear regression equation;  $y = -4.514x + 14.133$  with  $R^2 = 0.846$ . Past research observed that biodiesel with a shorter carbon chain ( $C_m:0, m \leq 16$ ) FAME (fatty acid methyl esters) would possess better cold flow properties, but if biodiesel contained more unsaturated FAME ( $C_m:1, m \leq 20$ ), the

biodiesel CFPP could be lower. Similarly, the number of double-bonds in FAMEs ( $C_m:n$ ,  $m \leq 22$ ,  $n \geq 1$ ) was better for biodiesel cold flow properties [37].

The addition of natural organic solvents (turpentine oil, diethyl ether, and n-butanol) to improve the cold flow behaviour of Neem biodiesel had no significant effect on the CFPP. However, increasing diethyl ether in fuel blends improved CFPP values with B10 and B20 blends (See Table 5). However, it should be noted that diethyl ether has a low flash point ( $-40^\circ\text{C}$ ) and instant evaporation at room temperature due to its reduced vapor pressure, making it challenging to use as a fuel additive. Furthermore, the calorific values of diethyl ether and n-butanol (33.8 MJ/kg and 33.2 MJ/kg, respectively) are excessively low, causing the fuel blends to operate with reduced brake power and torque. As a result, the biodiesel mix (B20T10) with turpentine oil and diesel can be used as additives with justified cold flow qualities.

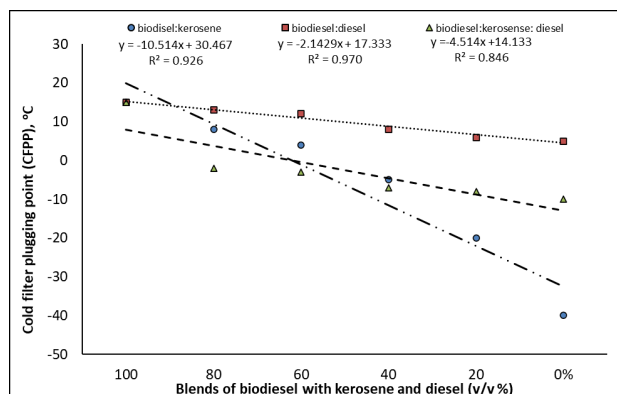


**Fig. 4.** Effect of Neem biodiesel ratio on CFPP of biodiesel: kerosene, biodiesel: diesel and biodiesel:kerosene:diesel blends.

#### 3.4.4. FTIR analysis of Neem biodiesel and its blends

FAME (fatty acid methyl ester) concentration is essential for quality. It provides an actual concentration in blending ratios of diesel blends that can be detected by FTIR (Fourier-transform infrared spectroscopy). Because FAME has a strong infrared absorption at around  $1745\text{ cm}^{-1}$  (due to the ester carbonyl bond), a region where fossil diesel is transparent, infrared spectroscopy is ideally suited to this analysis [38]. Fig. 5 presents FTIR spectra of biodiesel, kerosene, diesel, and a mixture of kerosene/diesel blends. Similarities and differences in absorbance peaks of these spectra help confirming the presence of main functional groups found in biodiesel. Neem biodiesel showed characteristic prominent peaks at  $1740.2\text{ cm}^{-1}$  denoting  $C=O$ , i.e., carbonyl group, which confirms the presence of es-

ter linkage. Another typical peak of biodiesel due to its  $O-CH_3$  stretching was found at  $1169\text{ cm}^{-1}$ . Confirmation of the ester functional group in the biodiesel from ATR-FTIR spectral peaks is in accordance with previous studies. Past research work by Patchimpet et al. described peaks at  $1743\text{ cm}^{-1}$ ,  $1744\text{ cm}^{-1}$  and  $1169\text{ cm}^{-1}$  as characteristics of ester in commercial biodiesel [39]. FTIR spectra of all three blends also contain methyl ester peaks at  $1744\text{ cm}^{-1}$ , and  $1169\text{ cm}^{-1}$ . However, the infrared spectrum of the kerosene and diesel does not have carbonyl groups. In addition, FTIR spectra of biodiesel, kerosene, and diesel have few similar peaks for example, prominent peaks were observed from  $2,845$  to  $2,970\text{ cm}^{-1}$  were due to the symmetric and asymmetric stretch of  $-CH$ ,  $-CH_2$ ,  $-CH_3$  of saturated hydrocarbons. A  $-CH$ ,  $-CH_3$  asymmetric deformation of aliphatic hydrocarbon chain brings about absorbance at around  $1460\text{ cm}^{-1}$  and  $1375\text{ cm}^{-1}$  while, at  $1358\text{ cm}^{-1}$  and  $1436\text{ cm}^{-1}$ ,  $CH_3$ , and  $CH_2$  methylene-bridge carbon were found, respectively. The peak obtained at around  $720\text{ cm}^{-1}$  was due to the stretching vibration of  $(CH_2)_n$  overlapping [40]. Fig. 6, ATR-FTIR absorption spectra of biodiesel, diesel, turpentine, diethyl ether, and n-butanol blends were found in the range from  $600\text{ cm}^{-1}$  to  $3500\text{ cm}^{-1}$ .

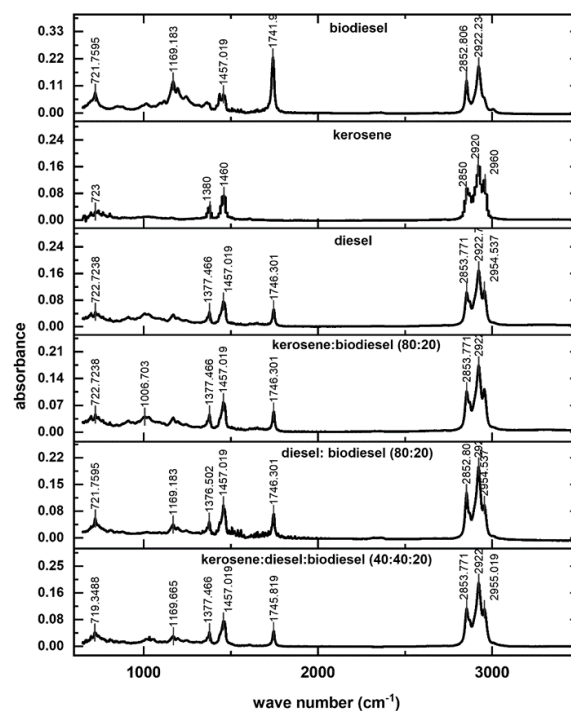


**Fig. 5.** ATR-FTIR absorption spectra of biodiesel, kerosene, diesel, kerosene: biodiesel (80:20) blend, diesel: biodiesel (80:20) blend and kerosene: diesel: biodiesel (40:40:20) blend in the range of  $600\text{ cm}^{-1}$ - $3500\text{ cm}^{-1}$ .

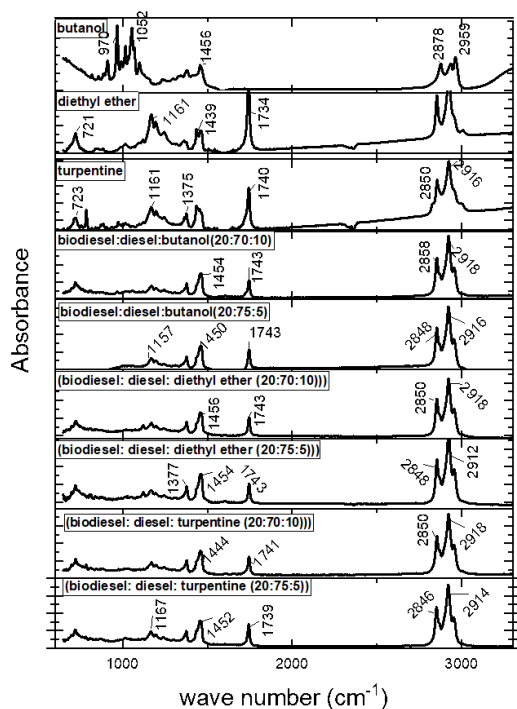


**Fig. 6.** ATR-FTIR absorption spectra of biodiesel, diesel, turpentine, diethyl ether and butanol blends in the range of  $600\text{ cm}^{-1}$ – $3500\text{ cm}^{-1}$

#### 3.4.5. Cost analysis of biodiesel production

The economic feasibility of Neem biodiesel is important to compete with petroleum-derived diesel. Biodiesel feedstocks contributes to around 75% of its overall cost. Therefore, selecting locally available cheap raw material is important for ensuring low cost of biodiesel produced and having favourable cold flow properties competitive with the mineral diesel [41]. Biodiesel production cost was calculated (see Table 7), where input cost was calculated as PKR.322.06 per L (USD 1.80 per L), incorporating the cost of chemicals and utilities used in its production. However, the total generated revenue from glycerol produced as a byproduct and methanol recovery cost was calculated as PKR. 205.04 per L (USD 1.14 per L). The net amount of biodiesel cost per L was found by the difference of total input cost on its production and the revenue generated as PKR 117.02 per L (USD 0.654 per L). The cost of blended biodiesel (B20), (B20\*), (B20\*\*) and (B20T10) were calculated as PKR 117.02 (USD 0.621), PKR 133.54 (USD 0.747), PKR 122.03 (USD 0.684) and PKR 139.78 (USD 0.782) per L, respectively. The cost of B20\*\* and B20T10 blends were

comparable to mineral diesel market price (USD 0.770)/L.

**Biodiesel production energy balance:** The net energy balance was calculated to be 0.1428. (i.e., 14.28 % net positive energy balance). Though the energy balance is favorable, it might be improved by lowering the cost of Neem oil as a feedstock by cultivating more Neem trees on marginal lands, yielding more raw oil, and utilizing solar thermal energy during biodiesel production.

#### 4. Conclusion

Two-step acid-base reactions were used to produce Neem biodiesel, and its analysis revealed qualities that were in line with international biodiesel standards. However, to enrich its poor cold flow behaviour to run diesel engines in moderate cold winters, Neem biodiesel with blends of kerosene, mineral diesel, mixed kerosene/ diesel, and natural turpentine oil resulted in no starvation, crystallization and gum formation. The blended sample with mixed kerosene and diesel (B20\*\*) showed improved CP, PP, and CFPP to  $-4.5\text{ }^{\circ}\text{C}$ ,  $-7\text{ }^{\circ}\text{C}$ , and  $-8\text{ }^{\circ}\text{C}$ , respectively, for its use in CI engines due to acceptable calorific value ( $49.58\text{ MJ/kg}$ ) and low viscosity ( $2.75\text{ mm}^2/\text{s}$ ) of mixtures. Similarly, B20T10 fuel blends showed better enhancement in low-temperature flow behaviour of Neem biodiesel with CP, PP, and CFPP to  $7\text{ }^{\circ}\text{C}$ ,  $5\text{ }^{\circ}\text{C}$  and  $-2\text{ }^{\circ}\text{C}$ , respectively. The existence of the ester compound was observed with FTIR spectra at  $1740.2\text{ cm}^{-1}$  ( $\text{C}=\text{O}$  ester). Also, its composition showed the presence of palmitic acid methyl ester, trans-methyl oleate, dimethyl oleate, and methyl stearate. The cost of producing Neem biodiesel, B20\*\* and B20T10 was USD 0.621/L, 0.684 /L, and 0.782/L, respectively. Neem biodiesel costs can be made even cheaper by massive plantation of Neem in marginal areas and using solar thermal energy in its production. Produced Neem biodiesel had a positive net energy balance of 14.28%. Based on the results of this study, it is recommended that B20\*\* and B20T10 to be used to run CI engines during cold weather without sacrificing fuel quality and at a lower cost than mineral diesel.

#### Acknowledgement

The authors are grateful to the NED University of Engineering and Technology Karachi, Pakistan, for providing laboratory facility and support in order to complete this research study. It is mentioned that there are no ethical standards of research involved in this manuscript and it is devoid of any conflict of interest. The authors would also like to acknowledge the University of Malaya and the Ministry of Higher Education Malaysia for helping through

**Table 7.** Cost estimation of biodiesel production from two step transesterification of Neem oil.

Materials and Utilities	Quantity consumed	Unit	Cost / Unit	Area fraction	Cost in PKR/ L
Neem oil	1	L	Rs.100/L	-	100
Methanol (20% by volume of oil)	0.2	L	Rs.1036/L	-	207.2
Sulphuric Acid (H <sub>2</sub> SO <sub>4</sub> )	0.01	L	Rs.1000/L	-	10
NaOH (1% per L of oil)	1.467 x10 <sup>-5</sup>	kg	Rs.200/kg	-	0.0029
Processing (heating / stirring) electricity consumption	2.275	kwh	Rs.18/kwh*	0.1187	4.860
× operating time 3.5 hours					
(a) Total biodiesel production cost (PKR per L) = 322.064					
Generated revenue					
Glycerol product (10% by volume)	0.1	L	Rs. 600/L	-	60
Methanol recovery (70% by volume)	0.14	L	Rs.1036/L	-	145.04
(b) Total generated revenue (PKR per L) = 205.04					
Net cost of Neem biodiesel produced Rs. per L (a-b) = 117.024 (USD 0.654) **					
Cost analysis of B20 blended with kerosene, diesel, and mixed kerosene / diesel ratios					
B20	B20*	B20**	B20T10		
23.448 + 87.624	23.448 + 110.096	23.448 + 43.812 + 55.048	23.448 + 96.334 + 20		
Rs / L = 111.07 (USD0.621)	Rs / L = 133.54 (USD0.747)	Rs / L = 122.30 (USD0.684)	Rs / L = 139.78 (USD0.782)		

\*K-Electric tariff charges [32]

\*\* Cost conversion from PKR into US\$ (1 USD= Rs.178.67)

the Fundamental Research Grant Scheme FP142-2019A- (FRGS/1/2019/TK03/UM/01/1).

## Nomenclature

API	American Petroleum Institute
ASTM	American Standard for Testing Materials
B10T10	10% biodiesel + 80% diesel + 10% turpentine
B20	20% biodiesel+80% kerosene
B20*	20% biodiesel+80% diesel
B20**	20% biodiesel + 40% kerosene + 40% diesel
B20T10	20% biodiesel + 70% diesel + 10% turpentine
CFPP	Cold filter plugging point
CI	Compression ignition
CO	Carbon monoxide
CO <sub>2</sub>	Carbon dioxide
CP	Cloud point
DEE	Diethyl ether
EN	European Standard
FAME	Fatty acid methyl ester
FTIR	Fourier transform infrared spectroscopy
HC	Hydrocarbons
KOH	Potassium hydroxide
L	Litres
NaOH	Sodium hydroxide
NO <sub>x</sub>	Nitrogen oxides
PCSIR	Pakistan Council for Scientific and Industrial Research
PKR	Pakistani rupees
PP	Pour point
rpm	revolutions per minute
TP	Turpentine oil
USD	United State Dollar

## References

- [1] P. Verma, M. Sharma, and G. Dwivedi, (2016) "Evaluation and enhancement of cold flow properties of palm oil and its biodiesel" **Energy Reports** 2: 8–13.
- [2] H. Yang, X.-H. Li, M.-F. Mu, G.-Y. Kou, et al., (2017) "Comparative performance and emissions study of a direct injection diesel engine using diesel fuel and soybean biodiesel" **Journal of Applied Science and Engineering** 20(2): 201–210.
- [3] G. Kumari and S. K. Karmee. "Thermochemical routes applying biomass: a critical assessment". In: *Handbook of Biofuels*. Elsevier, 2022, 435–451.
- [4] C. Campbell, (1992) "The depletion of oil" **Marine and petroleum geology** 9(6): 666–671.
- [5] C. A. L. Cardoso, M. E. Machado, and E. B. Caramão, (2016) "Characterization of bio-oils obtained from pyrolysis of bocaiuva residues" **Renewable Energy** 91: 21–31.
- [6] K. Abed, M. Gad, A. El Morsi, M. Sayed, and S. A. Elyazeed, (2019) "Effect of biodiesel fuels on diesel engine emissions" **Egyptian journal of petroleum** 28(2): 183–188.
- [7] S. Bhatia. *Advanced renewable energy systems, (Part 1 and 2)*. CRC Press, 2014.

- [8] G. Dwivedi and M. Sharma, (2014) "Impact of cold flow properties of biodiesel on engine performance" **Renewable and Sustainable Energy Reviews** 31: 650–656.
- [9] M. Ali, B. Naqvi, and I. A. Watson, (2018) "Possibility of converting indigenous *Salvadora persica* L. seed oil into biodiesel in Pakistan" **International Journal of Green Energy** 15(7): 427–435.
- [10] M. Serrano, R. Oliveros, M. Sánchez, A. Moraschini, M. Martinez, and J. Aracil, (2014) "Influence of blending vegetable oil methyl esters on biodiesel fuel properties: oxidative stability and cold flow properties" **Energy** 65: 109–115.
- [11] P. Berman, S. Nizri, and Z. Wiesman, (2011) "Castor oil biodiesel and its blends as alternative fuel" **biomass and bioenergy** 35(7): 2861–2866.
- [12] A. Demirbaş, (2008) "Production of biodiesel from algae oils" **Energy Sources, Part A: Recovery, Utilization, and Environmental Effects** 31(2): 163–168.
- [13] S. Nainwal, N. Sharma, A. S. Sharma, S. Jain, and S. Jain, (2015) "Cold flow properties improvement of *Jatropha curcas* biodiesel and waste cooking oil biodiesel using winterization and blending" **Energy** 89: 702–707.
- [14] J. Milano, H. C. Ong, H. Masjuki, W. Chong, M. K. Lam, P. K. Loh, and V. Vellayan, (2016) "Microalgae biofuels as an alternative to fossil fuel for power generation" **Renewable and Sustainable Energy Reviews** 58: 180–197.
- [15] P. Pramanik, P. Das, and P. Kim, (2012) "Preparation of biofuel from argemone seed oil by an alternative cost-effective technique" **Fuel** 91(1): 81–86.
- [16] L. Wen, Y. Wang, D. Lu, S. Hu, and H. Han, (2010) "Preparation of KF/CaO nanocatalyst and its application in biodiesel production from Chinese tallow seed oil" **Fuel** 89(9): 2267–2271.
- [17] A. I. El-Batal, A. A. Farrag, M. A. Elsayed, and A. M. El-Khawaga, (2016) "Biodiesel production by *Aspergillus niger* lipase immobilized on barium ferrite magnetic nanoparticles" **Bioengineering** 3(2): 14.
- [18] M. Hazrat, M. G. Rasul, M. Mofijur, M. Khan, F. Djanroodi, A. Azad, M. M. Bhuiya, and A. Silitonga, (2020) "A mini review on the cold flow properties of biodiesel and its blends" **Frontiers in Energy Research** 8: 598651.
- [19] I. Monirul, H. Masjuki, M. Kalam, N. Zulkifli, H. Rashedul, M. Rashed, H. Imdadul, and M. Mosarof, (2015) "A comprehensive review on biodiesel cold flow properties and oxidation stability along with their improvement processes" **RSC advances** 5(105): 86631–86655.
- [20] A. A. Mohammed, A. R. Al-Obaidi, and A. A. AlTabbakh. "Experimental investigation of using kerosene-biodiesel blend as an alternative fuel in diesel engines". In: *Journal of Physics: Conference Series*. 1279. 1. IOP Publishing. 2019, 012022.
- [21] P. Yogesh, D. Chandramohan, et al., (2022) "Combustion, Performance and Emissions Characteristics of CRDI engine Fueled with Biodiesel, Ethanol & Butanol blends at Various Fuel Injection strategies" **Journal of Applied Science and Engineering** 25(6): 971–977.
- [22] P. Dubey and R. Gupta, (2018) "Influences of dual bio-fuel (*Jatropha* biodiesel and turpentine oil) on single cylinder variable compression ratio diesel engine" **Renewable Energy** 115: 1294–1302.
- [23] L. Karikalan and M. Chandrasekaran, (2017) "Performance and pollutants analysis on diesel engine using blends of *Jatropha* Biodiesel and Mineral Turpentine as fuel" **International Journal of Environmental Science and Technology** 14(2): 323–330.
- [24] S. Sivalakshmi and T. Balusamy, (2013) "Effect of biodiesel and its blends with diethyl ether on the combustion, performance and emissions from a diesel engine" **Fuel** 106: 106–110.
- [25] M. Lapuerta, J. Rodríguez-Fernández, D. Fernández-Rodríguez, and R. Patiño-Camino, (2018) "Cold flow and filterability properties of n-butanol and ethanol blends with diesel and biodiesel fuels" **Fuel** 224: 552–559.
- [26] L. Karikalan and M. Chandrasekaran, (2017) "Performance and pollutants analysis on diesel engine using blends of *Jatropha* Biodiesel and Mineral Turpentine as fuel" **International Journal of Environmental Science and Technology** 14(2): 323–330.
- [27] M. H. Ali, M. Mashud, M. R. Rubel, and R. H. Ahmad, (2013) "Biodiesel from Neem oil as an alternative fuel for Diesel engine" **Procedia Engineering** 56: 625–630.
- [28] H. J. Berchmans and S. Hirata, (2008) "Biodiesel production from crude *Jatropha curcas* L. seed oil with a high content of free fatty acids" **Bioresource technology** 99(6): 1716–1721.

- [29] M. Mofijur, H. Masjuki, M. Kalam, M. Rasul, A. E. Atabani, M. Hazrat, and H. Mahmudul, (2015) "Effect of biodiesel-diesel blending on physico-chemical properties of biodiesel produced from *Moringa oleifera*" **Procedia Engineering** 105: 665–669.
- [30] G. Dwivedi and M. P. Sharma, (2015) "Investigation and improvement in cold flow properties of *Pongamia biodiesel*" **Waste and Biomass Valorization** 6(1): 73–79.
- [31] M. Ali and I. A. Watson, (2014) "Comparison of oil extraction methods, energy analysis and biodiesel production from flax seeds" **International journal of energy research** 38(5): 614–625.
- [32] K-Electric. *K-Electric schedule of electricity tariff 2020*. 2020.
- [33] P. S. Oil. *Petroleum Oil Lubricants.* Pakistan State Oil. 2020.
- [34] S. Banik, M. Rouf, T. Rabeya, M. Khanam, S. Sajal, S. Sabur, and M. Islam, (2018) "Production of biodiesel from neem seed oil" **Bangladesh Journal of Scientific and Industrial Research** 53(3): 211–218.
- [35] M. H. M. Yasin, R. Mamat, O. M. Ali, A. F. Yusop, M. A. Hamidi, M. Y. Ismail, and M. Rasul, (2017) "Study of diesel-biodiesel fuel properties and wavelet analysis on cyclic variations in a diesel engine" **Energy procedia** 110: 498–503.
- [36] D. Alviso, E. Saab, P. Clevenot, and S. D. Romano, (2020) "Flash point, kinematic viscosity and refractive index: variations and correlations of biodiesel–diesel blends" **Journal of the Brazilian Society of Mechanical Sciences and Engineering** 42(6): 1–15.
- [37] C. Yang, K. He, Y. Xue, Y. Li, H. Lin, and H. Sheng, (2018) "Factors affecting the cold flow properties of biodiesel: Fatty acid esters" **Energy Sources, Part A: Recovery, Utilization, and Environmental Effects** 40(5): 516–522.
- [38] B. Perston, N. Harris, and U. Seer Green, (2009) "Biodiesel Blend Analysis by FT-IR (ASTM D7371 and EN 14078)" **Application Note. FT-IR Spectroscopy. PerkinElmer, Inc. Seer Green, UK:**
- [39] J. Patchimpet, B. K. Simpson, K. Sangkharak, and S. Klomklao, (2020) "Optimization of process variables for the production of biodiesel by transesterification of used cooking oil using lipase from Nile tilapia viscera" **Renewable Energy** 153: 861–869.
- [40] P. de la Mata, A. Dominguez-Vidal, J. M. Bosque-Sendra, A. Ruiz-Medina, L. Cuadros-Rodriguez, and M. J. Ayora-Cañada, (2012) "Olive oil assessment in edible oil blends by means of ATR-FTIR and chemometrics" **Food Control** 23(2): 449–455.
- [41] D. Bolonio, A. Llamas, J. Rodriguez-Fernandez, A. M. Al-Lal, L. Canoira, M. Lapuerta, and L. Gomez, (2015) "Estimation of cold flow performance and oxidation stability of fatty acid ethyl esters from lipids obtained from *Escherichia coli*" **Energy & Fuels** 29(4): 2493–2502.